Available online at www.sciencedirect.com

ScienceDirect

www.elsevier.com/locate/jes

JES JOURNAL OF ENVIRONMENTAL SCIENCES

www.jesc.ac.cn

Simultaneous removal of Cu(II) and Cr(VI) by Mg–Al–Cl layered double hydroxide and mechanism insight

Xianyang Yue[1], *Weizhen Liu*[2,*], *Zuliang Chen*[3], *Zhang Lin*[1,2,**]

1. *Key Laboratory of Design and Assembly of Functional Nanostructures, Fujian Institute of Research on the Structure of Matter, Chinese Academy of Sciences, Fujian 350002, China. E-mail: xyyue@fjirsm.ac.cn*
2. *School of Environment and Energy, South China University of Technology, Guangdong 510006, China*
3. *Centre for Environmental Risk Assessment and Remediation, University of South Australia, Mawson Lakes, SA 5095, Australia*

ARTICLE INFO

Article history:
Received 25 September 2015
Revised 27 January 2016
Accepted 29 January 2016
Available online 4 March 2016

Keywords:
Adsorption
Heavy metals
Layered double hydroxide
Anion exchange
Precipitation

ABSTRACT

Mg–Al–Cl layered double hydroxide (Cl-LDH) was prepared to simultaneously remove Cu(II) and Cr(VI) from aqueous solution. The coexisting Cu(II) (20 mg/L) and Cr(VI) (40 mg/L) were completely removed within 30 min by Cl-LDH in a dosage of 2.0 g/L; the removal rate of Cu(II) was accelerated in the presence of Cr(VI). Moreover, compared with the adsorption of single Cu(II) or Cr(VI), the adsorption capacities of Cl-LDH for Cu(II) and Cr(VI) can be improved by 81.05% and 49.56%, respectively, in the case of coexisting Cu(II) (200 mg/L) and Cr(VI) (400 mg/L). The affecting factors (such as solution initial pH, adsorbent dosage, and contact time) have been systematically investigated. Besides, the changes of pH values and the concentrations of Mg^{2+} and Al^{3+} in relevant solutions were monitored. To get the underlying mechanism, the Cl-LDH samples before and after adsorption were thoroughly characterized by X-ray powder diffraction, transmission electron microscopy, Fourier transform infrared spectroscopy, and X-ray photoelectron spectroscopy. On the basis of these analyses, a possible mechanism was proposed. The coadsorption process involves anion exchange of Cr(VI) with Cl^- in Cl-LDH interlayer, isomorphic substitution of Mg^{2+} with Cu^{2+}, formation of $Cu_2Cl(OH)_3$ precipitation, and the adsorption of Cr(VI) by $Cu_2Cl(OH)_3$. This work provides a new insight into simultaneous removal of heavy metal cations and anions from wastewater by Cl-LDH.

Introduction

Electroplating wastewater generally contains highly toxic and carcinogenic anion Cr(VI) as well as many cations, such as Pb(II), Cu(II), Cd(II), which pose a great threat to both human health and ecological environment (Algarra et al., 2005; Panayotova et al., 2007). Numerous methods, including chemical precipitation, electro-chemical treatment, ion-exchange, membrane filtration, and adsorption technologies (Fu and Wang, 2011), have been used to remove these heavy metal ions from wastewater. Among them, chemical precipitation produces large amount of sludge, which may result in a problem of secondary contamination. Electro-chemical treatment expends a lot of electric energy. Additionally, ion-exchange and membrane filtration cannot be

* *Corresponding author.*
** *Corresponding author at: Key Laboratory of Design and Assembly of Functional Nanostructures, Fujian Institute of Research on the Structure of Matter, Chinese Academy of Sciences, Fujian 350002, China.*
E-mails: weizhliu@scut.edu.cn (Weizhen Liu), zlin@fjirsm.ac.cn (Zhang Lin).

http://dx.doi.org/10.1016/j.jes.2016.01.015
1001-0742/

used at large scale due to their high cost. On the contrary, adsorption technology appears to be an efficient and economic method for the removal of heavy metals from electroplating wastewater owing to the advantages of low cost, facile operation and regeneration of adsorbents (Agouborde and Navia, 2009; Fu and Wang, 2011; Guo et al., 2010; Jiang et al., 2010).

Nanomaterials, used as adsorbents to remove heavy metal ions from wastewater, have received significant attention owing to their high specific surface area (Hua et al., 2012; Khin et al., 2012). As one of them, layered double hydroxides (LDHs), with a general formula of $[M^{2+}_{1-x}M^{3+}_{x}(OH)_2]^{x+}$ $(A^{n-})_{x/n}\cdot yH_2O$ (Cavani et al., 1991), have been considered as one of the most promising adsorbents for removing highly concentrated toxic anions (such as CrO_4^{2-}, AsO_4^{2-}, and F^-) due to their high ionic exchange capacities (Goh et al., 2008; Türk et al., 2009; Wen et al., 2013). Specifically, the anions are mainly extracted through ionic exchange with anions in the interlayer of LDHs (Goh et al., 2008; Türk et al., 2009). In recent years, the utilization of LDHs to remove the toxic anions have been extensively investigated, involving the synthesis of LDHs with various morphologies (Li et al., 2014b; Tokudome et al., 2013; Yu et al., 2012), the adsorption thermodynamics and kinetics (Li et al., 2009), the factors affecting the adsorption efficiency (Goh et al., 2008; Guo et al., 2013), and the regeneration of adsorbents (Lv et al., 2013). Moreover, many reports have demonstrated that LDHs can also remove the metal cations, such as Hg^{2+}, Cd^{2+}, Pb^{2+}, Cu^{2+}, Zn^{2+}, Co^{2+}, Ni^{2+}, and Sr^{2+} (Fang and Chen, 2014; Goncharuk et al., 2011; Gong et al., 2011; Kameda et al., 2011; Ma et al., 2014; Park et al., 2007; Pavlovic et al., 2009; Vlad et al., 2014, 2015). The adsorption mechanism of cations by LDHs is based on surface precipitation of metal hydroxides, surface complexation through bonding with surface hydroxyl groups of LDHs, isomorphic substitution, and chelation with anion ligand in the interlayer of LDHs (Liang et al., 2013).

In spite of numerous studies on LDHs to remove heavy metal ions, few reports have been found for the simultaneous removal of these cations and anions, such as Cu(II) and Cr(VI), by LDHs. Considering the fact that cations and anions have different physical and chemical properties in aqueous solution, it is important to understand the influence of coexisting cations and anions on the removal efficiency of them by LDHs, which may provide a new insight into removal of coexisting contaminants. Recently, a Zn–Al LDH modified with chromotropic acid (CTA) was reported (Chen and Song, 2013), exhibiting a high selection and removal efficiency of Cu(II) and Cr(VI) from mixed metal ions, while the removal mechanism was not discussed clearly. Moreover, considering the high-cost of CTA, the modified LDH may not be suitable for large-scale treatment of industrial electroplating wastewater. Therefore, it is essential, on one hand, to explore LDHs with low cost (for instance, simple anions such as Cl^-, NO_3^-, and CO_3^{2-} intercalated LDHs) to achieve high removal efficiency of coexisting inorganic contaminants, and on the other hand, to figure out the interaction between coexisting cations/anions and the LDHs during the adsorption to further understand the removal mechanism.

In this study, Cl^- intercalated LDH, Mg–Al–Cl LDH (labeled as Cl-LDH) nanoflakes were facilely prepared through a coprecipitation method and was used to remove coexisting Cu(II)–Cr(VI) from aqueous solution. We aimed to understand the simultaneous removal behavior of coexisting Cu(II) and Cr(VI) by Cl-LDH. Therefore, the main objectives are: (1) comparing the removal efficiency and adsorption capacity between coexisting Cu(II)–Cr(VI) and single Cu(II) or Cr(VI), (2) studying the changes of solution pH and Cl-LDH before and after removal of coexisting Cu(II)–Cr(VI) by using various characterization techniques, (3) figuring out the mechanism for simultaneous removal of coexisting Cu(II)–Cr(VI) by Cl-LDH. This work confirms the high efficiency of Cl-LDH to remove coexisting heavy metal cations and anions and provides a new insight into the relative mechanism.

1. Materials and methods

1.1. Preparation of Mg–Al–Cl LDH

All reagents used in this study were of analytical grade and used without further purification. The Cl-LDH was synthesized through a coprecipitation method based on a previous study (Lv et al., 2013). In brief, a mixed aqueous solution of $MgCl_2\cdot6H_2O$ and $AlCl_3\cdot6H_2O$ was prepared with a Mg/Al molar ratio of 3:1 (total cation concentration of 0.5 mol/L). Afterwards, 6 mol/L NaOH was dropwise added into the mixed solution under stirring until the final pH value of the resultant suspension was adjusted to 9.5. The white precipitate was aged for 2 hr in the parent solution at room temperature. After filtration, the precipitate was collected and washed with deionized water for several times, and then dried at 110°C overnight. The whole synthesis process did not use inert atmosphere so as to simplify the preparation condition and get ready for the practical application of Cl-LDH in electroplating wastewater treatment.

1.2. Adsorption experiments

Single Cu(II) with an initial concentration of 20 and 200 mg/L, single Cr(VI) with an initial concentration of 40 and 400 mg/L, and coexisting Cu(II)–Cr(VI) solutions with an initial concentration of 60, 100, 200, and 400 mg/L for Cu(II) and 100, 200, 400, 800 mg/L for Cr(VI) were prepared by dissolving $Cu(NO_3)_2\cdot3H_2O$ and $K_2Cr_2O_7$ into deionized water, respectively. 0.1 g Cl-LDH powder was added into 50 mL Cu(II), Cr(VI) and coexisting Cu(II)–Cr(VI) solutions under stirring, respectively. The initial pH values of the solutions were adjusted to 3.8 with 1 mol/L HCl and 1 mol/L NaOH solution. Then 0.5–1.5 mL solution was extracted and filtered at a certain time interval to test the residual concentration of Cu(II) or Cr(VI) by an atomic absorption spectrophotometer (AAS) (AA240, Varian, USA) equipped with an air-acetylene flame. The removal efficiency (R, %) of Cu(II) or Cr(VI), was calculated by the following Eq. (1):

$$R = (C_0 - C_t)/C_0 \times 100\% \quad (1)$$

where, C_0 (mg/L) is the initial concentration of Cu(II) or Cr(VI) in the solution, C_t (mg/L) is the concentration of Cu(II) or Cr(VI) at time t (min) of adsorption.

To monitor the change of pH values of solution during adsorption, 50 mL Cu(II), Cr(VI), and coexisting Cu(II)–Cr(VI) with the initial concentration of 20 mg/L for Cu(II) and 40 mg/L for Cr(VI) as well as blank (without heavy metal) solutions were

prepared with an initial pH value of 3.8 adjusted by 1 mol/L HCl, and followed by adding 0.1 g Cl-LDH powder into the four solutions, respectively. Then the pH values were recorded with a pH meter at different time intervals. After adsorption, 4–5 mL solutions were extracted and filtered to test the concentrations of Mg^{2+} and Al^{3+} in filtrates by an inductively coupled plasma atomic emission spectrometry (ICPAES) (Ultima2, Jobin Yvon, France). The Cl-LDH after adsorption was collected by centrifugation and washed for three times with deionized water, then dried at 100°C overnight.

1.3. Characterization

The synthesized Cl-LDH samples before and after adsorption of single Cu(II), single Cr(VI) and coexisting Cu(II)–Cr(VI) with different initial concentrations were characterized.

X-ray diffraction (XRD) was used to identify the phase composition and crystal structure of the samples. Diffraction data were recorded on an X' Pert PRO diffractometer (PANalytical, Netherlands) with Cu Kα radiation (λ = 0.15406 nm) at 40 kV and 40 mA. The diffraction angle 2θ varied from 5° to 85° with a scanning speed of 4°/min in a continuous mode.

To identify the chemical formula of the synthesized Cl-LDH, an Oxford-INCA energy-dispersive X-ray spectroscopy (EDS) (JSM6700-F, JEOL, Japan) was used to semi-quantitatively analyze the metal irons of Cl-LDH. The Mg and Al contents of the synthesized Cl-LDH were determined by ICPAES after the sample was dissolved in 1 mol/L HCl. The C and H contents of the synthesized Cl-LDH were determined by CHN elemental analyzer (Vario EL-Cube, Elementar, Germany). Thermogravimetric analysis (TGA) and differential thermal analysis (DTA) of the Cl-LDH were performed using a Thermo-Analyzer System (STA 449C, NETZSCH, Germany) in the temperature range of 25–1000°C at a heating rate of 10°C/min in flowing nitrogen gas. The infrared spectra of the samples were recorded on a PerkinElmer Spectrum 100 Fourier transform infrared spectrometer (FT-IR) (USA) using KBr pellets in the range of 4000–400 cm^{-1}.

Transmission electron microscopy (TEM) was used to observe the morphology and size of the samples. The TEM imaging was conducted on a FEI field-emission transmitting electron microscope (Tecnai F20, USA) at an acceleration voltage of 200 kV.

An Oxford-INCA energy-dispersive X-ray spectroscopy (EDS) (JSM6700-F, JEOL, Japan) was used for the elemental analysis of the metal irons after adsorption.

X-ray photoelectron spectroscopy (XPS) measurements were performed on a Thermo Scientific ESCALAB 250 instrument with Al Kα source. All the binding energies were referenced to the C 1s peak of the surface adventitious carbon at 284.6 eV.

2. Results and discussion

2.1. Characterization of Cl-LDH

Fig. 1 shows the typical XRD pattern, TEM image, FT-IR spectrum, and TG-DTA curves of the synthesized Cl-LDH. As can be seen in Fig. 1a, the XRD pattern presents three characteristic basal reflections of a typical hydrotalcite-like material with a series of symmetric (00l) peaks at lower 2θ values. The interlayer spacing of (003) plane (d_{003}) at 2θ = 11.3° is 0.7852 nm, and d_{006} at 2θ = 22.7° is 0.3920 nm, which is consistent with the report in other literature (Özgümüş et al., 2013). The prepared Cl-LDH is non-uniform flake shape with a particle size below 100 nm according to the TEM image (Fig. 1b). Besides, EDS data (Appendix A Fig. S1a) reveals that the Cl-LDH mainly consists of Mg, Al, O, Cl, and C elements. To further identify relative specific functional groups, FT-IR spectrum of Cl-LDH was measured, as shown in Fig. 1c. The broad bands at 3466 and 1636 cm^{-1} are associated with the stretching vibrations of OH group in the brucite-like layer and bending vibration of water molecules in the interlayer. The bands at 1372 and 842 cm^{-1} are due to the vibration mode of CO_3^{2-}, which may be introduced into the interlayer of Mg–Al LDH by absorption of CO_2 during the preparation procedure (Li et al., 2014a; Li et al., 2009). The bands between 400 and 800 cm^{-1} are attributed to the characteristic lattice vibrations of MgO and Al_2O_3. Therefore, it confirms the presence of intercalated Cl^-, CO_3^{2-}, and water molecules in LDH interlayer.

The chemical formula of synthesized Cl-LDH was estimated via ICPAES, CHN analyses, TG-DTA and charge balance considerations. The Mg and Al contents obtained from the ICPAES analysis are 453.22 and 155.72 mg/L, respectively. The C and H contents obtained from CHN analyses are 0.06% (W/W) and 4.14% (W/W), respectively. According to the TG-DTA curves (Fig. 1d), the weight loss between 110°C and 226°C was 10.97%, which is due to the elimination of interlayer structural water (Özgümüş et al., 2013). The weight loss between room temperature and 110°C is attributed to the evaporation of adsorbed water. On the basis of these data, the idealized chemical formula for the synthesized Mg–Al LDH was estimated to be: $[Mg_{0.76}Al_{0.24}(OH)_2]Cl_{0.18}(CO_3)_{0.03}{\cdot}0.42H_2O$.

2.2. Removal of Cu(II) and Cr(VI) by Cl-LDH

Solution pH is an important factor affecting the adsorption of metal ions. The initial pH of solution in the range of 2.0–8.0 was used to investigate its effect on the adsorption capacity of Cl-LDH with respect to Cu(II) and Cr(VI) under the condition of coexisting Cu(II) (20 mg/L) and Cr(VI) (40 mg/L). As shown in Fig. 2, the adsorption capacities of Cl-LDH with respect to both Cu(II) and Cr(VI) are favored in an initial pH range from 4.0 to 6.0, with the optimal pH of 4.0. When the pH value is from 2.0 to 3.0, a part of Cl-LDH may be dissolved because of the high concentrations of H^+ (Li et al., 2009), leading to a less adsorption of both Cu(II) and Cr(VI). At higher pH value of 7.0–8.0, most of Cu(II) is hydrolyzed and precipitated as $Cu(OH)_2$ (Dean, 1992) before adding Cl-LDH, causing very little adsorption of Cu(II). In addition, the precipitation presents yellow color, indicating that the formed $Cu(OH)_2$ may adsorb Cr(VI), reducing the amount of Cr(VI) for the absorption by Cl-LDH. In view of the common pH value of 2.0–4.0 for industrial wastewater, the initial pH of 3.8 of solution is used throughout the following batch experiments.

The residual concentration and removal efficiency of Cu(II) and Cr(VI) for aqueous solution containing single Cu(II) (20 mg/L) or Cr(VI) (40 mg/L) or with coexisting Cu(II) (20 mg/L) and Cr(VI) (40 mg/L) at different adsorption times are shown in Fig. 3. As can be seen, Cl-LDH with a dosage of 2.0 g/L can effectively remove Cr(VI) from aqueous solution with single Cr(VI), achieving a complete removal within 20 min. In contrast,

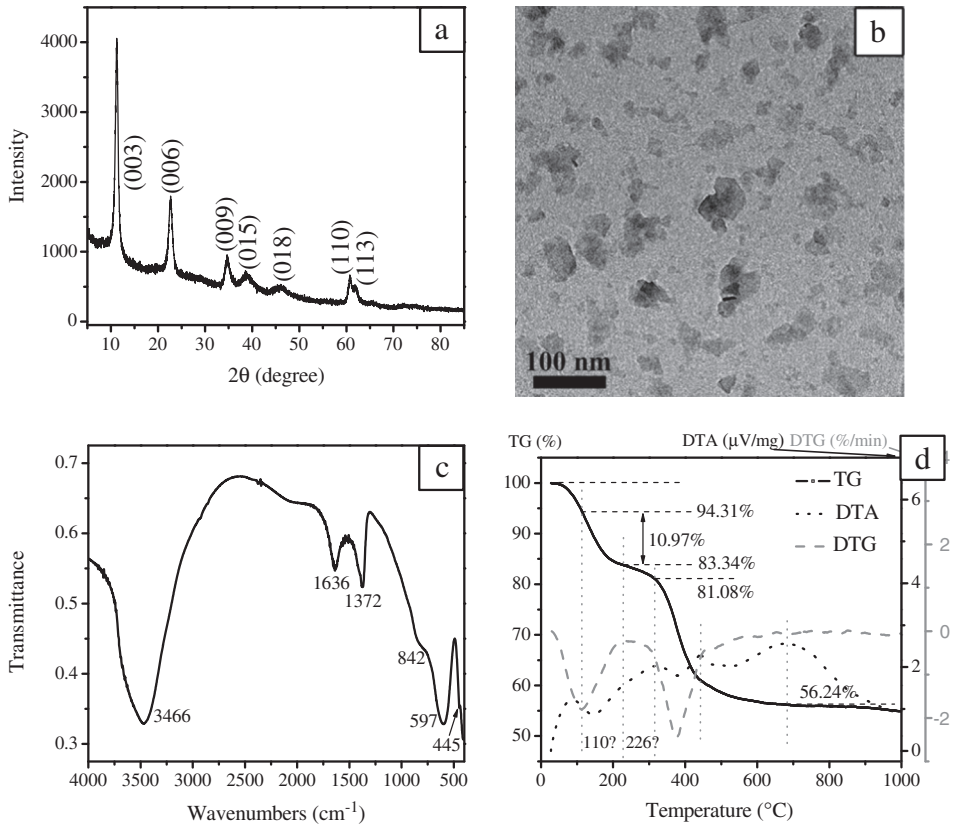

Fig. 1 – X-ray powder diffraction (XRD) pattern (a), transmission electron microscopy (TEM) image (b), Fourier transform infrared spectroscopy (FT-IR) spectrum (c), and thermogravimetric analysis and differential thermal analysis (TG-DTA) curves (d) of Cl-LDH prepared by the coprecipitation method.

the removal rate of Cu(II) from aqueous solution with single Cu(II) is much slower, reaching equilibrium within 50 min with removal efficiency of 99.3%. Interestingly, in the case of coadsorption of Cu(II) and Cr(VI), the removal rate of Cu(II) is accelerated obviously. In other words, the presence of Cr(VI) can accelerate the removal rate of Cu(II) from aqueous solution. 99.4% of Cu(II) as well as Cr(VI) are removed within 30 min, indicating the effectiveness of Cl-LDH in simultaneous removal of Cu(II) and Cr(VI) at low initial concentrations.

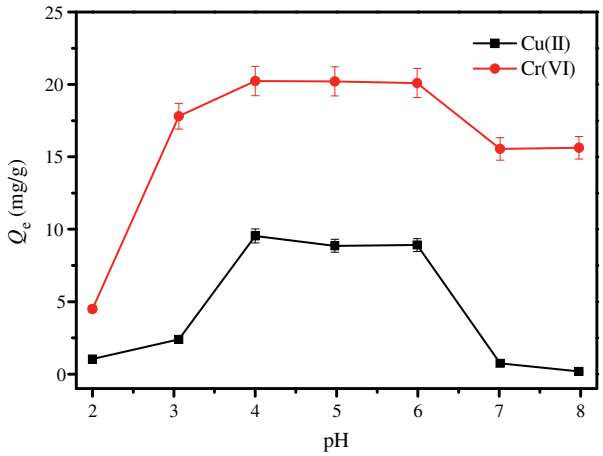

Fig. 2 – Effect of solution initial pH on the adsorption capacity of Cl-LDH with respect to Cu(II) and Cr(VI) under the condition of coexisting Cu(II) (20 mg/L) and Cr(VI) (40 mg/L). Cl-LDH dosage: 0.1 g, solution volume: 50 mL, equilibration time: 2 hr, temperature: 15°C.

Moreover, a fixed amount of Cl-LDH dosage (2.0 g/L) and varying concentrations of coexisting Cu(II) and Cr(VI) were used to investigate the effect of adsorbent dosage and contact time on the adsorption capacity of Cl-LDH towards Cu(II) and Cr(VI), as shown in Fig. 4. In the case of single Cu(II) (200 mg/L), the adsorption of Cu(II) does not reach equilibrium yet after 120 min, showing a slow removal rate. As for single Cr(VI) (400 mg/L), the adsorption of Cr(VI) reaches equilibrium within 30 min in association with a maximum adsorption capacity of 45.20 mg/g, but the removal efficiency of Cr(VI) is only 28.2%. In contrast, both adsorption capacity and removal rate are obviously enhanced in the case of coadsorption of Cu(II) and Cr(VI). In general, the adsorption capacities of Cl-LDH towards Cu(II) and Cr(VI) increase with the increasing initial concentration. As shown in Fig. 4a, the adsorption of Cu(II) reaches equilibrium within 30 min when the initial concentrations of Cu(II) are 60 and 100 mg/L, and tends to reach equilibrium after 120 min when the initial concentrations of Cu(II) are 200 and 400 mg/L, in association with a removal efficiency of 99.99%, 97.12%, 95.36%, and 69.53% respectively, indicating that the Cl-LDH with the dosage of 2.0 g/L approximately reaches saturate adsorption when the initial concentration of Cu(II) is more than 200 mg/L. Similarly, as seen in Fig. 4b, the adsorption

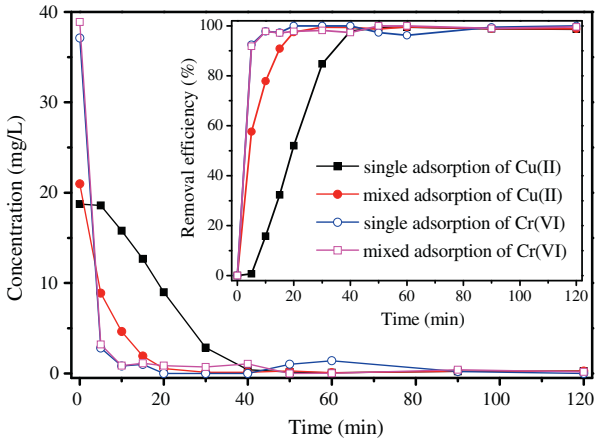

Fig. 3 – Comparison of residual concentration and removal efficiency (the inset) of Cu(II) and Cr(VI) by Cl-LDH in single Cu(II), single Cr(VI) and coexisting Cu(II)–Cr(VI) solutions at different adsorption time. Cl-LDH dosage: 0.1 g, solution volume: 50 mL, Cu(II) = 20 mg/L, Cr(VI) = 40 mg/L, initial pH = 3.8, temperature: 30°C.

of Cr(VI), in the case of coexisting Cu(II) and Cr(VI), also reaches equilibrium within 30 min when the initial concentrations of Cr(VI) are 100 and 200 mg/L, and the removal efficiency of Cr(VI) are 80.99% and 53.38%, respectively. This implies that the Cl-LDH with the dosage of 2.0 g/L has reached saturate adsorption when the initial concentration of Cr(VI) is more than 100 mg/L. The maximum adsorption capacity of Cl-LDH is 143.85 mg/g towards Cu(II) and 112.70 mg/g towards Cr(VI) in the case of coexisting Cu(II) (400 mg/L) and Cr(VI) (800 mg/L).

To clarify the removal behavior of Cl-LDH for coadsorption of Cu(II) and Cr(VI), various techniques were used to characterize the Cl-LDH before and after adsorption. The XRD patterns of LDH samples before and after adsorption of single/coexisting Cu(II) and Cr(VI) with different initial concentrations are shown in Fig. 5, and the corresponding interlayer space of typical peaks at lower 2θ values are listed in Table 1. At low concentrations, either single adsorption of Cu(II) (20 mg/L) or Cr(VI) (40 mg/L) or coadsorption of 20 mg/L Cu(II) and 40 mg/L Cr(VI) makes (003) and (006) peaks of Cl-LDH slightly shift to lower 2θ values, indicating a slightly larger interlayer space. For Cl-LDH with 20 mg/L Cu(II), this may suggest the isomorphic substitution of Mg^{2+} with Cu^{2+} for their close ionic size (0.066 nm for Mg^{2+} and 0.072 nm for Cu^{2+}) (Fang and Chen, 2014; Gong et al., 2011), leading to the increase of brucite-like layer width. In the case of Cl-LDH with 40 mg/L Cr(VI), it can be attributed to the anion exchange reaction between Cr(VI) and anions in the interlayer of Cl-LDH (Li et al., 2009; Lv et al., 2013), which enlarged the gallery height for the larger ionic size of Cr(VI) anion. It should be noted that the changes of the d_{001} values for Cl-LDH with 40 mg/L Cr(VI) were quite small. This may be related to the low content of new generating composition after adsorption, which is near the detection limit of XRD. As for simultaneous adsorption of Cu(II) and Cr(VI), the isomorphic substitution of Mg^{2+} with Cu^{2+} and the anion exchange reaction of Cr(VI) with anions in the interlayer of Cl-LDH may both occur, causing a maximum value of d_{003} and d_{006} compared with that of Cl-LDH with 20 mg/L Cu(II) and Cl-LDH with 40 mg/L Cr(VI).

To make the results more convinced, the XRD patterns of Cl-LDH after adsorption of high concentration of single Cu(II), single Cr(VI), and the coexisting Cu(II)–Cr(VI) (Fig. 5 and Appendix A Fig. S2) were also examined. The (003) and (006) peaks obviously shifted to lower 2θ values after the adsorption of high concentration of Cu(II), and botallackite, $Cu_2Cl(OH)_3$ (JCPDS No. 01-087-0679) formed as an additional phase. The result suggests the removal of Cu(II) by Cl-LDH may be through not only isomorphic substitution of Mg^{2+} with Cu^{2+}, but also the formation of $Cu_2Cl(OH)_3$ precipitation. After adsorption of high concentration of Cr(VI), the diffraction peaks of the sample become wider and less intense. Meanwhile, the (003) peak was down-shifted to the lower angle in comparison with Cl-LDH. The increase in basal spacing from 0.7852 to 0.8611 nm further indicates the intercalation of Cr(VI) anions into the interlayer of Cl-LDH (Lv et al., 2013). These results indicate that the simultaneous removal of Cu(II) and Cr(VI) by Cl-LDH are through: (1) anion exchange of Cr(VI)

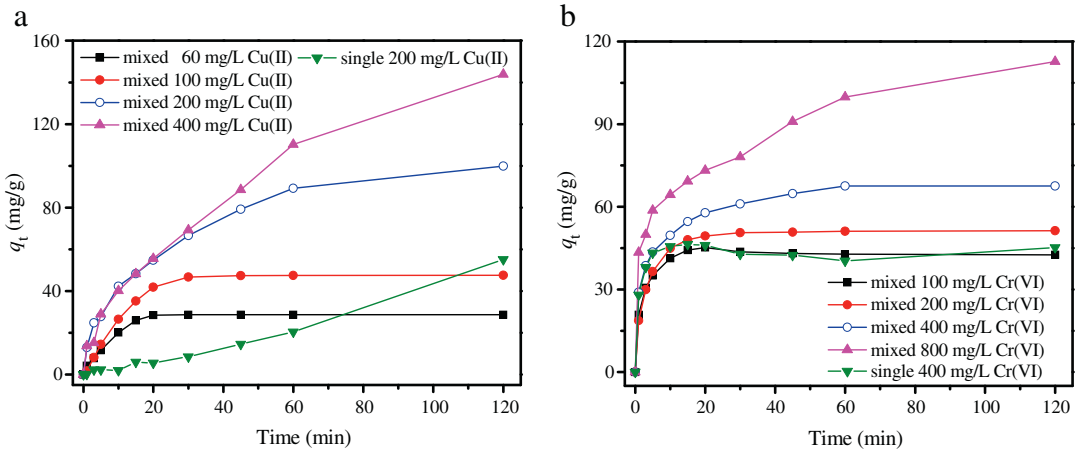

Fig. 4 – Effect of contact time on the adsorption capacity of Cu(II) (a) and Cr(VI) (b) by Cl-LDH at different initial concentrations of single/coexisting Cu(II) and Cr(VI). Cl-LDH dosage: 0.1 g, solution volume: 50 mL, initial pH = 3.8, temperature: 15°C.

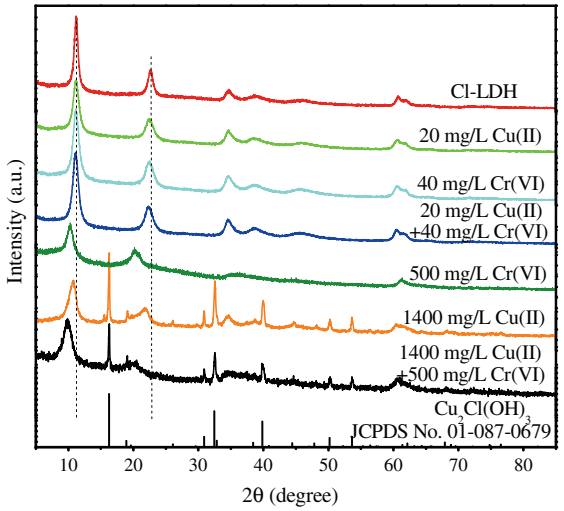

Fig. 5 – X-ray powder diffraction (XRD) patterns of Cl-LDH before and after adsorption of single/coexisting Cu(II) and Cr(VI) with different initial concentrations. Cl-LDH dosage: 0.1 g, solution volume: 50 mL, initial pH = 3.8.

with anion ions (Cl^- or OH^-) in the interlayer of Cl-LDH; (2) isomorphic substitution of Mg^{2+} with Cu^{2+}; (3) formation of $Cu_2Cl(OH)_3$ precipitation. In view of the adsorption behavior shown in Fig. 4, the adsorption of 200 mg/L mixed Cr(VI) has reached equilibrium under the Cl-LDH dosage of 2.0 g/L, while the improvement of adsorption capacity for higher concentration mixed Cr(VI) may be attribute to the surface adsorption of increased $Cu_2Cl(OH)_3$ precipitation.

In order to examine the surface morphology after adsorption, TEM images of Cl-LDH after adsorption of single Cu(II) (20 mg/L), single Cr(VI) (40 mg/L), and coexisting Cu(II) (20 mg/L) and Cr(VI) (40 mg/L) (labeled as Cl-LDH-Cu, Cl-LDH-Cr, and Cl-LDH-CuCr respectively) are presented in Fig. 6. Compared with original Cl-LDH, as can be seen, crimped membranes that piled together with smooth surface were formed after adsorption of Cu(II) (Fig. 6a). Besides, some tiny particles were also observed adhered to the membrane surface. HRTEM image (which is not shown in the present article) did not show the diffraction fringe of these particles, indicating the quite low crystallinity of them. Similar morphology of crimped membranes was also observed after adsorption of Cr(VI) (Fig. 6b), which may be the result of crystallization of Cl-LDH caused by the adsorption reaction. The intercalation of Cr(VI) into Cl-LDH interlayer may promote the exfoliation and reconstruction of Cl-LDH sheets, leading to the formation of a few thinner sheets piled together (Lv et al., 2013). For Cl-LDH-CuCr (Fig. 6c), the aggregated and crystallized membranes with tiny particles became bigger with a size of 280–850 nm, while the particles were still with poor crystallinity. To identify the specific contents of these particles, the elemental mappings of Mg, Al, Cu, and Cr for Cl-LDH-CuCr were elaborated, as shown in Fig. 6d. The results indicated the similar distribution of Cr with that of Mg and Al in the sample, and the distribution of Cu was mostly uniform and consistent with the basal distribution of Mg, which can be attributed to the isomorphic substitution of Mg^{2+} by Cu^{2+}. Besides, some bright dispersive spots in the mapping of Cu were also observed, as shown in the white circles, which correspond with the features of the tiny particles. The particles may be probably botallackite precipitation. This further suggests the intercalation of Cr(VI) into Cl-LDH, isomorphic substitution of Mg^{2+} with Cu^{2+}, and the formation of $Cu_2Cl(OH)_3$ particles deposited on the surface of Cl-LDH.

Identifying the elemental information by EDS confirms the metal ion adsorbed onto the Cl-LDH, as shown in Appendix A Fig. S1. Cu or Cr was detected after the adsorption of Cu(II) or Cr(VI), confirming the fixation of Cu(II) or Cr(VI) from low concentration of aqueous solution by Cl-LDH (Appendix A Fig. S1b and Fig. S1c). It is not surprising to note that both Cu and Cr were detected after the adsorption of coexisting Cu(II)–Cr(VI), which is consistent with the result of batch adsorption experiments. In addition, the content of Cl decreased from Mg/Al/Cl molar ratio of 3.30:1:0.84 for Cl-LDH to 3.25:1:0.55 for Cl-LDH-Cr and 3.18:1:0.35 for Cl-LDH-CuCr, to some degree, confirming the anion exchange between Cl^- and Cr(VI) during the adsorption of Cr(VI).

XPS was employed to study the fixed metal speciation to further determine the adsorption reaction of Cl-LDH during the removal of coexisting Cr(VI) and Cu(II), as shown in Fig. 7. The presence of Cu and Cr in fully scanned survey was obviously observed after adsorption (Fig. 7a). Besides, one more peak in O 1s high resolution spectra appeared, where the binding energy (E_B) value slightly shifted from 531.48 to 531.74 eV. This indicates the formation of new O–M bands, probably O–Cr or/and O–Cu. In addition, the E_B value of Mg 1s also remarkably shifted by 2.6 eV, implying an intense variation of Mg bonding environment. This is likely due to the entrance of strong oxidative Cr(VI) into the interlayer of Cl-LDH. The high resolution XPS spectrum of Cr 2p showed the peaks of $2p_{3/2}$ and $2p_{1/2}$ located at 579.53 and 588.53 eV (Fig. 7c), corresponding to Cr(VI) (Allen and Tucker, 1976). The Cu 2p peaks at 935.7, 943.4, 955.8, and 962.4 eV were also observed from the high resolution XPS spectrum (Fig. 7d), implying the formation of Cu hydroxides during the removal of Cu(II) (Fang and Chen, 2014). Besides, the increased E_B of Cu 2p3/2 (generally at 933.8 eV–935.1 eV for CuO and $Cu(OH)_2$ (Dake et al., 2000; McIntyre and Cook, 1975)) might suggest the combination of Cu^{2+} with oxidative Cr(VI) anions, and revealed the substitution of Cu^{2+} with Mg^{2+} as the substituted Cu^{2+} in the host of Cl-LDH-CuCr may bind with the Cr(VI) anions in interlayer. In addition, the atomic concentration ratios of Mg/Al/Cl for Cl-LDH and Cl-LDH-CuCr evaluated by XPS were 2.50:1:0.68 and 1.44:1:0.21, showing obvious decrease

Table 1 – Comparison of the d_{003} and d_{006} values obtained from XRD patterns of Cl-LDH before and after adsorption of single Cu(II), single Cr(VI) and coexisting Cu(II)–Cr(VI) with different initial concentrations.

Samples	Cl-LDH	Cl-LDH-Cu	Cl-LDH-Cr	Cl-LDH-CuCr	Cl-LDH-1400 Cu	Cl-LDH-500 Cr	Cl-LDH-1400 Cu + 500 Cr
d_{003} (nm)	0.7852	0.7882	0.7921	0.7946	0.8232	0.8611	0.8918
d_{006} (nm)	0.3923	0.3966	0.3964	0.3982	0.4070	0.4383	0.4426

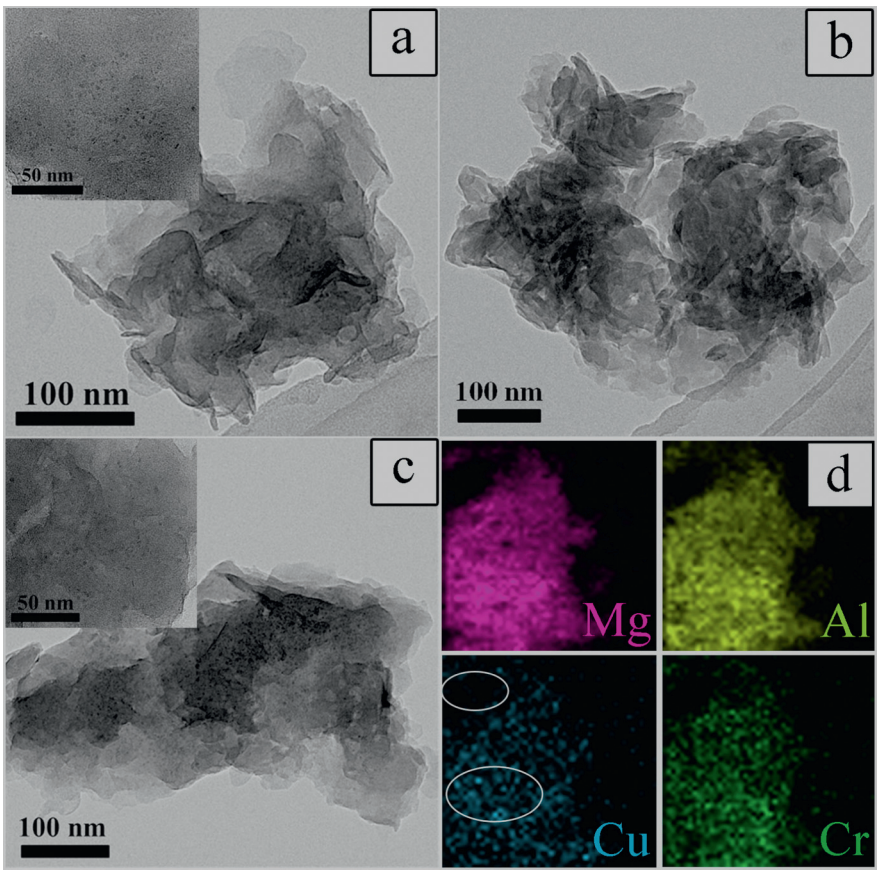

Fig. 6 – Transmission electron microscopy (TEM) images of Cl-LDH-Cu (a), Cl-LDH-Cr (b), Cl-LDH-CuCr (c), and elemental mappings of Mg, Al, Cu, and Cr (d) for Cl-LDH-CuCr. The inserts in (a) and (c) are enlarged TEM images of Cl-LDH-Cu and Cl-LDH-CuCr, respectively, showing the details of tiny particles adhered to the membrane surfaces.

of Mg and Cl compared with Al after the adsorption of coexisting Cu(II)–Cr(VI) solution. This result further confirms the isomorphic substitution of Mg^{2+} by Cu^{2+} and ion exchange of Cr(VI) with Cl^- in Cl-LDH.

FT-IR was further used to study the changes of some functional groups of Cl-LDH-Cu, Cl-LDH-Cr, and Cl-LDH-CuCr (Appendix A Fig. S3). In contrast with that of Cl-LDH, there was no obvious change of the spectrum for Cl-LDH-Cu except for that the bands corresponding to CO_3^{2-} became sharp and slightly shifted to 1384 and 839 cm^{-1} (Appendix A Fig. S3b). This may be due to the interaction of CO_3^{2-} in Cl-LDH interlayer with Cu^{2+} entranced into Cl-LDH layer through isomorphic substitution of Mg^{2+}. After adsorption of single Cr(VI) (Appendix A Fig. S3c) or coexisting Cu(II)–Cr(VI) (Appendix A Fig. S3d), the observed vibration band of CO_3^{2-} at 1375 or 1382 cm^{-1} indicated the existence of CO_3^{2-} in the interlayer of LDH. It may imply that there is not anion exchange reaction between CO_3^{2-} and Cr(VI) for the strength affinity of CO_3^{2-} to the interlayer of LDH (Radha et al., 2005). Besides, similar weak bands at 872 cm^{-1} were also observed for Cl-LDH-Cr and Cl-LDH-CuCr. The band is the characteristic infrared band of chromate corresponding to mode ν_d (Cr–O), which is recorded at 890 cm^{-1} for free chromate (Nakamoto, 1986). Relative slight shift of the band towards lower frequency may be due to the hydrogen bonding of Cr(VI) anion with interlayer water molecules or layer hydroxyl groups (Li et al., 2009).

From the above analysis, the simultaneous removal of Cu(II) and Cr(VI) in low concentration by Cl-LDH are probably through the following three ways: (1) anion exchange of Cr(VI) with Cl^- in the interlayer of Cl-LDH; (2) formation of $Cu_2(OH)_3Cl$ precipitation; (3) isomorphic substitution of Mg^{2+} with Cu^{2+}. Considering these reactions may lead to the change of pH values and Mg^{2+} and Al^{3+} concentrations in solution, the pH values of single Cu(II), Cr(VI), coexisting Cu(II)–Cr(VI), and blank (without heavy metal) solutions were monitored during adsorption and the concentrations of Mg^{2+} and Al^{3+} in the four solutions were analyzed by ICPAES after adsorption to further investigate the coadsorption mechanism. Relative results are shown in Fig. 8 and Table 2. As can be seen in Table 2, Mg^{2+} was detected in the blank solution, suggesting a partial dissolution of Cl-LDH at the initial pH of 3.8. This is consistent with the raising pH values of blank solution in Fig. 8. Considering the much smaller solubility product constants of $Al(OH)_3$ (K_{sp} = 1.3 × 10^{-33}, 25°C) compared with that of $Mg(OH)_2$ (K_{sp} = 1.8 × 10^{-11}, 25°C) (Dean, 1992), it is obviously reasonable for the detection of little Al^{3+}. A higher amount of Mg^{2+} released into single Cu(II) solution reveals that the isomorphic substitution of Mg^{2+} with Cu^{2+} also occurred in addition to the dissolution of Cl-LDH, for the source of Mg^{2+} in the solution only consisting of dissolution of Cl-LDH and isomorphic substitution by Cu^{2+}. Besides, based on the stoichiometric ratio, the amount of Cu^{2+} participating in isomorphic substitution reaction is 0.5740 mg (calculated by

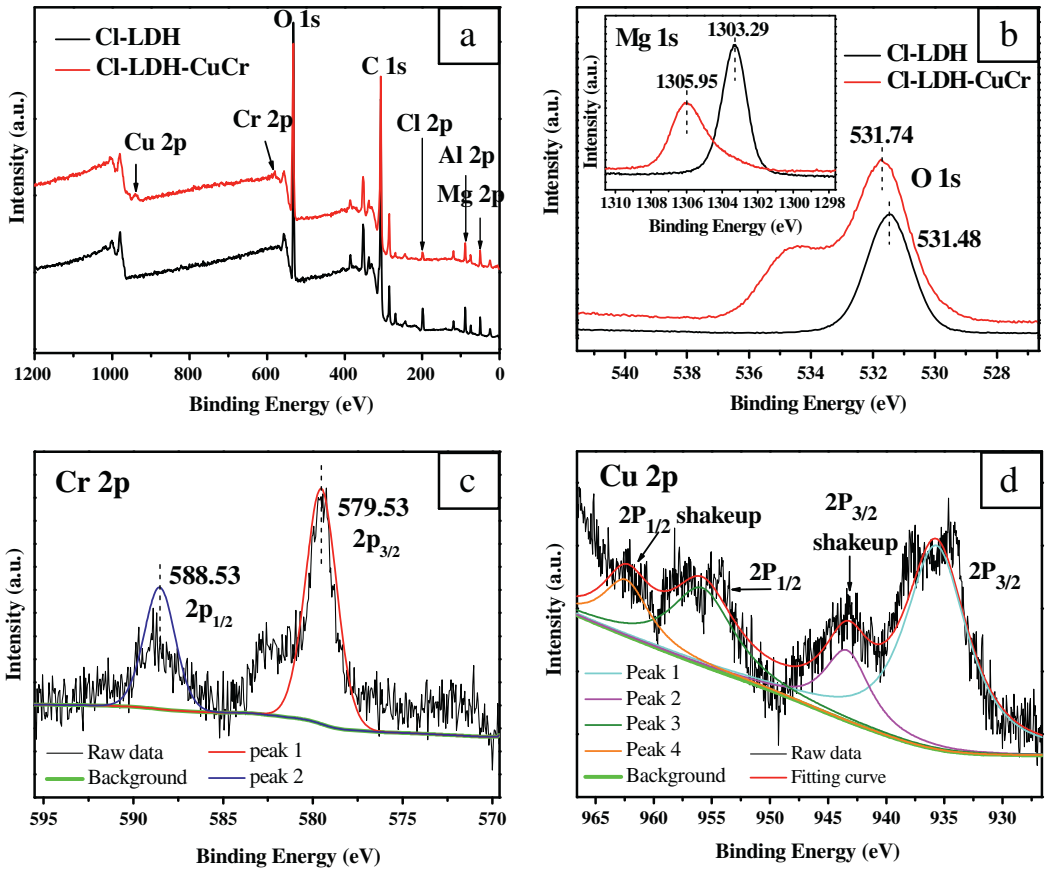

Fig. 7 – X-ray photoelectron spectroscopy (XPS) spectra of Cl-LDH and Cl-LDH-CuCr. (a) full survey, (b) O 1s and Mg 1s (the inset) high resolution XPS spectra, (c) Cr 2p high resolution XPS spectra of Cl-LDH-CuCr, and (d) Cu 2p high resolution XPS spectra of Cl-LDH-CuCr.

(26.180–14.700) × 0.05 mg = 0.5740 mg), which is less than the whole amount of Cu^{2+} immobilized from the single Cu(II) solution (20 × 0.05 mg = 1.00 mg). It implies the existence of another remove process by formation of $Cu_2Cl(OH)_3$ precipitation deposited on the surface of Cl-LDH, which weakened the protonation reaction of Cl-LDH (Li et al., 2009), leading to a lower pH values curve compared with that of blank solution. In the case of single Cr(VI) solution, the content of Mg^{2+} was also higher than that of blank solution. This may be because of the rapid anion exchange of Cr(VI) with Cl^- in Cl-LDH interlayer, promoting the exfoliation of Cl-LDH sheets and the dissolution of Cl-LDH layers, further resulting in the rapidly increase of pH values at the initial adsorption period. The study on the coexisting Cu(II)–Cr(VI) adsorption showed the maximum amount of Mg^{2+} discharged in the solution, suggesting the existence of both isomorphic substitution of Mg^{2+} with Cu^{2+} and dissolution of Cl-LDH caused by the rapid intercalation of Cr(VI) into Cl-LDH. The dissolution of Cl-LDH would cause fast consumption of H_3O^+ and the release of abundant hydration OH^- in the solution. Then the hydration OH^- and Cl^- released from the dissolution of Cl-LDH may react with Cu^{2+} to form $Cu_2Cl(OH)_3$ precipitation, which increased the removal rate of Cu(II) as observed in Fig. 3. As a result, the pH values of mixed solution were much smaller than that of single Cr(VI) solution while little larger compared with that of single Cu(II) and blank solution at the initial adsorption period.

2.3. Adsorption mechanism of coexisting Cu(II)–Cr(VI) by Cl-LDH

On the basis of all the above analyses, a possible adsorption mechanism of coexisting Cu(II)–Cr(VI) by Cl-LDH is proposed,

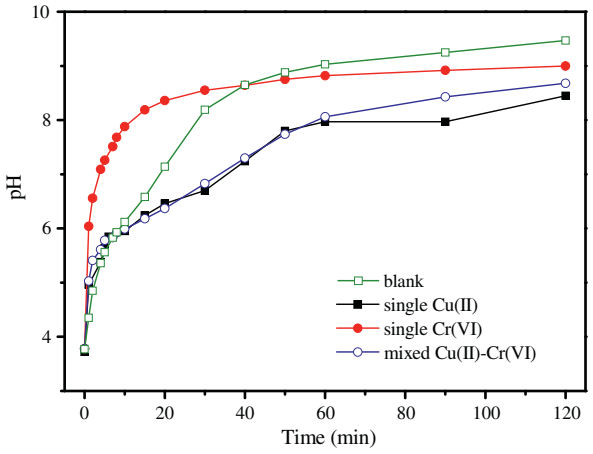

Fig. 8 – Comparison of pH values of single Cu(II), single Cr(VI) and coexisting Cu(II)–Cr(VI) solutions during the adsorption process. Cl-LDH dosage: 0.1 g, solution volume: 50 mL, Cu(II) = 20 mg/L, Cr(VI) = 40 mg/L, initial pH = 3.8.

Table 2 – Comparison of Mg^{2+} and Al^{3+} concentrations in the solutions after the adsorption of single Cu(II), single Cr(VI) and coexisting Cu(II)–Cr(VI) by Cl-LDH.

Samples	I-Cu	I-Cr	I-CuCr	$S_{Cl\text{-}LDH\text{-}Cu}$	$S_{Cl\text{-}LDH\text{-}Cr}$	$S_{Cl\text{-}LDH\text{-}CuCr}$	$S_{LDH\text{-}blank}$
Mg^{2+} (mg/L)	0.053	0.015	0.003	26.180	24.510	31.060	14.700
Al^{3+} (mg/L)	0.002	0	0.011	0.031	0.190	0.180	0.120

I-Cu, I-Cr, and I-CuCr present the initial solutions of single Cu(II), single Cr(VI) and coexisting Cu(II)–Cr(VI).
$S_{Cl\text{-}LDH\text{-}Cu}$, $S_{Cl\text{-}LDH\text{-}Cr}$, $S_{Cl\text{-}LDH\text{-}CuCr}$, and $S_{LDH\text{-}blank}$ present the solutions of single Cu(II), single Cr(VI), coexisting Cu(II)–Cr(VI) and blank after the adsorption by Cl-LDH.

as illustrated in Fig. 9. The process may be as follows: As Cl-LDH added into the solution, a fast and efficient ion exchange reaction of Cr(VI) with Cl^- in the interlayer of Cl-LDH occurred. At the same time, a partial of Cl-LDH dissolved for the initial high acidity of the solution and the rapid anion exchange of Cr(VI) with Cl^- in Cl-LDH interlayer, leading to the increase of solution pH and release of Cl^-. Then the Cl^- and partial hydration OH^- combined with the surrounding Cu^{2+} to form $Cu_2Cl(OH)_3$ precipitation deposited on the surface of Cl-LDH, promoting the removal rate of Cu^{2+}. Besides, $Cu_2Cl(OH)_3$ may also adsorb the residual Cr(VI) in high concentration, improving the adsorption capacity of Cl-LDH for Cr(VI) in gradient concentrations. Furthermore, Cu^{2+} was also partly fixed through isomorphic substitution of Mg^{2+} in the layer of Cl-LDH. The whole reactions can be described by Eqs. (2)–(6).

$$Cr(VI) + \text{Cl-LDH} \rightarrow \text{Cr(VI)-LDH} + Cl^- \quad (2)$$

$$H_3O^+ + \text{Cl-LDH} \rightarrow Mg^{2+} + Al^{3+} + Cl^- + CO_3^{2-} + H_2O \quad (3)$$

$$Cu^{2+} + Cl^- + H_2O \rightarrow Cu_2Cl(OH)_3\downarrow + H_3O^+ \quad (4)$$

$$Cu_2Cl(OH)_3 + Cr(VI) \rightarrow Cu_2Cl(OH)_3 \cdots Cr(VI) \quad (5)$$

$$Cu^{2+} + \text{Mg-LDH} \rightarrow \text{Cu-LDH} + Mg^{2+} \quad (6)$$

where Cr(VI)-LDH, Mg-LDH and Cu-LDH represent Cr(VI) intercalated Cl-LDH, original Cl-LDH, and substituted Cl-LDH with Cu(II) entranced into the layer, respectively.

3. Conclusion

This study demonstrates firstly that Mg–Al–Cl LDH is an efficient absorbent for the simultaneous removal of Cu(II) and Cr(VI) in different concentrations. The new findings include: (1) the adsorption of co-existing Cu(II) and Cr(VI) by Cl-LDH promotes the removal rate of Cu(II) while has no effect on the adsorption of Cr(VI) in low concentration (≤40 mg/L); (2) comparing with the adsorption of single Cu(II) or Cr(VI), the adsorption capacities of Cl-LDH with respect to Cu(II) and Cr(VI) can be improved by 81.05% and 49.56%, respectively, in the case of coexisting Cu(II) (200 mg/L) and Cr(VI) (400 mg/L). (3) the co-adsorption process involves anion exchange of Cr(VI) with Cl^- in the interlayer of Cl-LDH, isomorphic substitution of Mg^{2+} with Cu^{2+}, formation of $Cu_2Cl(OH)_3$ precipitation, and the adsorption of Cr(VI) by $Cu_2Cl(OH)_3$; (4) the hydration OH^- generated from the dissolution of Cl-LDH may accelerate the removal of Cu(II) through forming $Cu_2Cl(OH)_3$ precipitation, and meanwhile the precipitation may also improve the removal of Cr(VI) through surface adsorption. In summary, these new findings provide a new insight into the simultaneous removal of heavy metal cations and anions by LDH based on different adsorption mechanism.

Acknowledgments

This work was supported by the National Basic Research Program (973) of China (No. 2010CB933501), the National

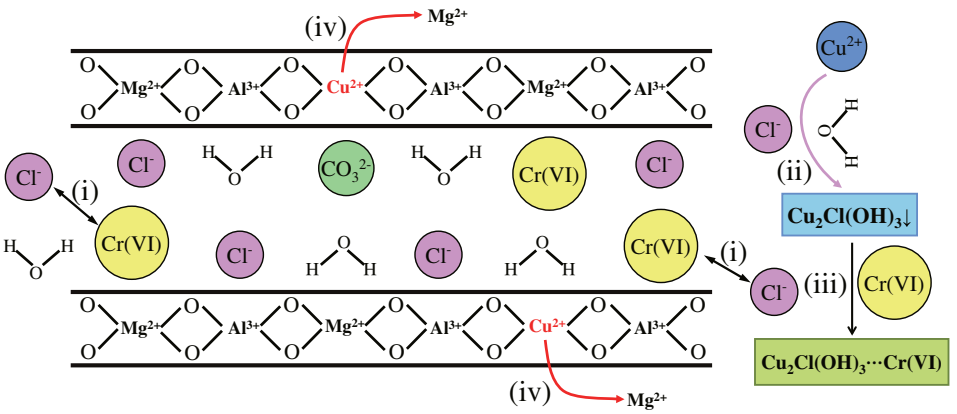

Fig. 9 – Schematic diagram of coadsorption mechanism of Cu(II) and Cr(VI) by Cl-LDH.

Natural Science Foundation of China (No. 21477128), and The National Science Fund for Distinguished Young Scholars (No. 21125730).

Appendix A. Supplementary data

Supplementary data to this article can be found online at http://dx.doi.org/10.1016/j.jes.2016.01.015.

REFERENCES

Agouborde, L., Navia, R., 2009. Heavy metals retention capacity of a non-conventional sorbent developed from a mixture of industrial and agricultural wastes. J. Hazard. Mater. 167 (1), 536–544.

Algarra, M., Jiménez, M.V., Rodríguez-Castellón, E., Jiménez-López, A., Jiménez-Jiménez, J., 2005. Heavy metals removal from electroplating wastewater by aminopropyl-Si MCM-41. Chemosphere 59 (6), 779–786.

Allen, G.C., Tucker, P.M., 1976. Multiplet splitting of X-ray photoelectron lines of chromium complexes. The effect of covalency on the 2p core level spin-orbit separation. Inorg. Chim. Acta 16, 41–45.

Cavani, F., Trifiro, F., Vaccari, A., 1991. Hydrotalcite-type anionic clays: Preparation, properties and applications. Catal. Today 11 (2), 173–301.

Chen, Y., Song, Y.F., 2013. Highly selective and efficient removal of Cr(VI) and Cu(II) by the chromotropic acid-intercalated Zn–Al layered double hydroxides. Ind. Eng. Chem. Res. 52 (12), 4436–4442.

Dake, L.S., King, D.E., Czanderna, A.W., 2000. Ion scattering and X-ray photoelectron spectroscopy of copper overlayers vacuum deposited onto mercaptohexadecanoic acid self-assembled monolayers. Solid State Sci. 2 (8), 781–789.

Dean, J.A., 1992. Lange's Handbook of Chemistry. 14th ed. McGraw-Hill, New York.

Fang, Q., Chen, B., 2014. Self-assembly of graphene oxide aerogels by layered double hydroxides cross-linking and their application in water purification. J. Mater. Chem. A 2 (23), 8941–8951.

Fu, F.L., Wang, Q., 2011. Removal of heavy metal ions from wastewaters: A review. J. Environ. Manage. 92 (3), 407–418.

Goh, K.H., Lim, T.T., Dong, Z.L., 2008. Application of layered double hydroxides for removal of oxyanions: A review. Water Res. 42 (6), 1343–1368.

Goncharuk, V., Puzyrnaya, L., Pshinko, G., Kosorukov, A., Demchenko, V.Y., 2011. Removal of Cu(II), Ni(II), and Co(II) from aqueous solutions using layered double hydroxide intercalated with EDTA. J. Water Chem. Technol. 33 (5), 288–292.

Gong, J.M., Liu, T., Wang, X.Q., Hu, X.L., Zhang, L.Z., 2011. Efficient removal of heavy metal ions from aqueous systems with the assembly of anisotropic layered double hydroxide nanocrystals@ carbon nanosphere. Environ. Sci. Technol. 45 (14), 6181–6187.

Guo, M.X., Qiu, G.N., Song, W.P., 2010. Poultry litter-based activated carbon for removing heavy metal ions in water. Waste Manage. 30 (2), 308–315.

Guo, Y., Zhu, Z., Qiu, Y., Zhao, J., 2013. Synthesis of mesoporous Cu/Mg/Fe layered double hydroxide and its adsorption performance for arsenate in aqueous solutions. J. Environ. Sci. 25 (5), 944–953.

Hua, M., Zhang, S.J., Pan, B.C., Zhang, W.M., Lv, L., Zhang, Q.X., 2012. Heavy metal removal from water/wastewater by nanosized metal oxides: A review. J. Hazard. Mater. 211–212, 317–331.

Jiang, M.Q., Jin, X.Y., Lu, X.Q., Chen, Z.L., 2010. Adsorption of Pb(II), Cd(II), Ni(II) and Cu(II) onto natural kaolinite clay. Desalination 252 (1), 33–39.

Kameda, T., Hoshi, K., Yoshioka, T., 2011. Uptake of Sc^{3+} and La^{3+} from aqueous solution using ethylenediaminetetraacetate-intercalated Cu–Al layered double hydroxide reconstructed from Cu–Al oxide. Solid State Sci. 13 (2), 366–371.

Khin, M.M., Nair, A.S., Babu, V.J., Murugan, R., Ramakrishna, S., 2012. A review on nanomaterials for environmental remediation. Energy Environ. Sci. 5 (8), 8075–8109.

Li, Y.J., Gao, B.Y., Wu, T., Sun, D.J., Li, X., Wang, B., et al., 2009. Hexavalent chromium removal from aqueous solution by adsorption on aluminum magnesium mixed hydroxide. Water Res. 43 (12), 3067–3075.

Li, L., Li, R.M., Gai, S.L., He, F., Yang, P.P., 2014a. Facile fabrication and electrochemical performance of flower-like Fe_3O_4@C@ layered double hydroxide (LDH) composite. J. Mater. Chem. A 2 (23), 8758–8765.

Li, Z., Yang, B., Zhang, S., Wang, B., Xue, B., 2014b. A novel approach to hierarchical sphere-like ZnAl-layered double hydroxides and their enhanced adsorption capability. J. Mater. Chem. A 2 (26), 10202–10210.

Liang, X.F., Zang, Y.B., Xu, Y.M., Tan, X., Hou, W.G., Wang, L., et al., 2013. Sorption of metal cations on layered double hydroxides. Colloids Surf. A Physicochem. Eng. Asp. 433, 122–131.

Lv, X.Y., Chen, Z., Wang, Y.J., Huang, F., Lin, Z., 2013. Use of high-pressure CO_2 for concentrating Cr^{VI} from electroplating wastewater by Mg–Al layered double hydroxide. ACS Appl. Mater. Interfaces 5 (21), 11271–11275.

Ma, S.L., Chen, Q.M., Li, H., Wang, P.L., Islam, S.M., Gu, Q.Y., et al., 2014. Highly selective and efficient heavy metal capture with polysulfide intercalated layered double hydroxides. J. Mater. Chem. A 2 (26), 10280–10289.

McIntyre, N., Cook, M., 1975. X-ray photoelectron studies on some oxides and hydroxides of cobalt, nickel, and copper. Anal. Chem. 47 (13), 2208–2213.

Nakamoto, K., 1986. Infrared and Raman Spectra of Inorganic and Coordination Compounds. John Wiley & Sons, New York.

Özgümüş, S., Gök, M.K., Bal, A., Güçlü, G., 2013. Study on novel exfoliated polyampholyte nanocomposite hydrogels based on acrylic monomers and Mg–Al–Cl layered double hydroxide: Synthesis and characterization. Chem. Eng. J. 223, 277–286.

Panayotova, T., Dimova-Todorova, M., Dobrevsky, I., 2007. Purification and reuse of heavy metals containing wastewaters from electroplating plants. Desalination 206 (1), 135–140.

Park, M., Choi, C.L., Seo, Y.J., Yeo, S.K., Choi, J., Komarneni, S., et al., 2007. Reactions of Cu^{2+} and Pb^{2+} with Mg/Al layered double hydroxide. Appl. Clay Sci. 37 (1), 143–148.

Pavlovic, I., Pérez, M., Barriga, C., Ulibarri, M., 2009. Adsorption of Cu^{2+}, Cd^{2+} and Pb^{2+} ions by layered double hydroxides intercalated with the chelating agents diethylenetriamine pentaacetate and meso-2, 3-dimercaptosuccinate. Appl. Clay Sci. 43 (1), 125–129.

Radha, A.V., Vishnu Kamath, P., Shivakumara, C., 2005. Mechanism of the anion exchange reactions of the layered double hydroxides (LDHs) of Ca and Mg with Al. Solid State Sci. 7 (10), 1180–1187.

Tokudome, Y., Tarutani, N., Nakanishi, K., Takahashi, M., 2013. Layered double hydroxide (LDH)-based monolith with interconnected hierarchical channels: Enhanced sorption affinity for anionic species. J. Mater. Chem. A 1 (26), 7702–7708.

Türk, T., Alp, I., Deveci, H., 2009. Adsorption of As(V) from water using Mg–Fe-based hydrotalcite (FeHT). J. Hazard. Mater. 171 (1), 665–670.

Vlad, A., Birjega, R., Matei, A., Luculescu, C., Mitu, B., Dinescu, M., et al., 2014. Retention of heavy metals on layered double hydroxides thin films deposited by pulsed laser deposition. Appl. Surf. Sci. 302, 99–104.

Vlad, A., Birjega, R., Matei, A., Luculescu, C., Nedelcea, A., Dinescu, M., et al., 2015. Detection of copper ions from aqueous solutions using layered double hydroxides thin films deposited by PLD. Appl. Surf. Sci. 352, 184–188.

Wen, T., Wu, X.L., Tan, X.L., Wang, X.K., Xu, A.W., 2013. One-pot synthesis of water-swellable Mg–Al layered double hydroxides and graphene oxide nanocomposites for efficient removal of As(V) from aqueous solutions. ACS Appl. Mater. Interfaces 5 (8), 3304–3311.

Yu, X.Y., Luo, T., Jia, Y., Xu, R.X., Gao, C., Zhang, Y.X., et al., 2012. Three-dimensional hierarchical flower-like Mg–Al-layered double hydroxides: highly efficient adsorbents for As(V) and Cr(VI) removal. Nanoscale 4 (11), 3466–3474.